Stator End-winding Currents in Frequency-domain Dielectric Response Measurements

N. Taylor and H. Edin
School of Electrical Engineering
KTH (Royal Institute of Technology)
Teknikringen 33,
10044 Stockholm, Sweden

ABSTRACT

This is a study of the components of capacitance, loss and harmonic currents that the nonlinear 'corona protection' coating used on stator end-windings adds to frequency-domain dielectric measurements. The work is based on measurements on simple laboratory models, compared to one-dimensional numerical models having discrete or continuous parameters and linear or nonlinear resistance. The necessary components and parameters of the numerical models are discussed by comparison with the measurements. Commonly used models of the conductivity of the SiC-based nonlinear material are compared to dc measurements on samples. The studied range of the applied voltage has amplitudes from low values up to the levels of operation and testing of stator windings, and frequency from line-frequency down to millihertz.

Index Terms — **Rotating machine insulation testing, stress control, dielectric measurements, capacitance measurement, loss measurement.**

1 INTRODUCTION

IN the end-windings (overhang) of high-voltage stators a nonlinear resistive stress-grading material is applied to the insulation surface for some centimetres beyond the point where the slot semiconductor layer ends, in order to limit the electric field in the surrounding air or other gas. The geometry and nonlinearity of the applied material cause additional capacitance, loss and harmonic currents to be measured in the insulation system, with strong dependence on the amplitude and frequency of the applied voltage. There is no practical way of 'guarding' these currents out of measurements made on a whole stator, which has typically hundreds of bar-ends emerging from the core.

Common measurements of the 'tip-up' of loss-tangent or capacitance with increasing voltage [1], or of the change in capacitance and loss with varied frequency [2], involve changes that are small proportions of the total current in the stator insulation. The end-winding currents correspond to a capacitance, loss and harmonics that are strongly dependent on the amplitude and frequency of the applied voltage. Although the graded parts are a modest part of the total length of each bar, they can strongly influence the variations with voltage and frequency. The end-winding currents therefore cause a considerable disturbance to these types of diagnostic measurement.

Partial discharges (PD) within a stator winding cause currents that can be included in dielectric measurements; detection of this PD current is a major purpose of the tip-up tests already mentioned. The modeling described in this paper arose from an interest in frequency-domain dielectric spectroscopy (FD-DS) on stator insulation, with the applied voltage varied over a range of amplitudes and low frequencies. The total current due to PD activity is included in such measurements: by measuring harmonics as well as fundamental-frequency components in the current, the phase-distribution of PD charge can be seen, and the PD current can be distinguished from the larger but approximately linear currents in the insulation's capacitance. The stress-grading, being strongly nonlinear as well as frequency-dependent, is the main source of disturbance to these harmonic components in the current.

If the current in the end-winding can be modeled sufficiently to allow most of it to be subtracted from the measured results, this would improve the accuracy of the tip-up tests and of FD-DS measurements of the insulation material and PD currents. It may even be desirable to check the correct functioning of the stress-grading by comparing measurements to expected parameter-limits.

Previous work with models of stress-grading has been oriented more to design than to diagnostic measurements. The interest is therefore on stress-distribution and heating effects rather than on currents, and on frequencies in the kilohertz range rather than the millihertz range. This is seen in the references about material models, cited in section 4.1. Frequency-domain dielectric response measurements on stator insulation at high voltage and low frequency are not common practice, but they are useful if PD is one of the phenomena of interest; time-domain measurements are more widely used, but transformation between time and frequency in the presence of strong nonlinearities is not likely to give useful results. Work not involving a wide range of voltages

Manuscript received on 15 January 2010, in final form 12 April 2010.

and frequencies, or done before the time of inexpensive computer simulation, makes use of approximations whose error it would be good to be able to assess and probably to avoid. The aim here is to see what features of voltage and frequency dependence the stress-grading current has over the ranges of interest in dielectric response measurements, and what models of the material and grading give a reasonable description of this.

2 CYLINDRICAL LABORATORY-MODELS

Simple gradings were made in the laboratory to study as purely as possible the effects of the grading material and geometry. A PTFE (polytetrafluoroethylene, Teflon™) tube was fitted tightly around a longer metal pipe, and an outer electrode of copper tape was applied for a short distance along the middle of the tube's length. The surface of the tube beyond the outer electrode was coated with one of two types of commercial stress-grading material for stator end-windings, a paint and a tape; more detail about the materials and how they were applied can be found in section 4. Two such bars are shown in Figure 1, and their construction and dimensions are shown in Figure 2.

Figure 1. Pictures of simple stress-graded model bars using B-stage tape (top) or corona-protection paint (bottom). The total length is about 0.5 m.

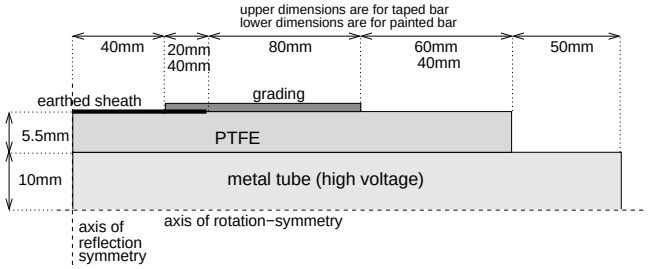

Figure 2. One side of an axisymmetric section of the bars depicted in Figure 1. Two of the dimensions vary between the bars with paint and with tape: both bars' dimensions are then shown.

The cylindrical shape was chosen for convenience of assembly and for easy analysis. The PTFE insulation was chosen for ease of handling, tolerance of the required curing-temperature for resin-based grading tapes, and for its low dispersion in our frequency range such that it can reasonably be regarded as having a fixed permittivity. The two-ended construction was used to prevent PD or leakage current that could occur if one end were left open. The middle section with the copper tape electrode was used to allow the manufacturer-prescribed overlap distance of the stress-grading material along the electrode, and to give a realistic field-distribution around the start of the grading.

Two bars were made for of each of the two materials, as a simple check of variance. There was not a strong difference seen in the behavior of the duplicates: the taped ones were very similar, and the painted ones had variation that would easily be explained by the variation of the paint's thickness that is seen in Figure 6. Only results from a taped bar are shown in this paper, as the tape had more consistent properties and a rather higher conductance that caused more of the details of the response to occur in a convenient frequency-range. The painted bars' responses were of similar shape but were shifted at least a decade lower in frequency.

3 SPECTROSCOPY RESULTS

Frequency-domain dielectric measurements were made on the laboratory models using the IDA200 instrument and its external 30 kV amplifier, from Programma (now Megger) of Täby, Sweden. A bar was suspended in the air, and one end of the inner tube was connected to the high-voltage supply. The measurement cable leading to the instrument's electrometer was connected to the middle of the outer conductor. The IDA200 instrument applies a sinusoidal voltage, and samples the applied voltage and the current at 16 kHz, recording for each of the DFT (discrete fourier-transform) components from the fundamental frequency up to the eighth harmonic.

3.1 FUNDAMENTAL-FREQUENCY COMPONENTS OF CURRENT

A sinusoidal voltage was applied to the central metal tube, with frequency varied from 100 Hz down to 10 mHz, and amplitude varied from 1.5 kV to 15.3 kV. The fundamental-frequency components (harmonic order 1, the same frequency as the applied voltage) of current in the two ends of the grading are shown in Figure 3, scaled to the familiar form of capacitance C' and loss C''.

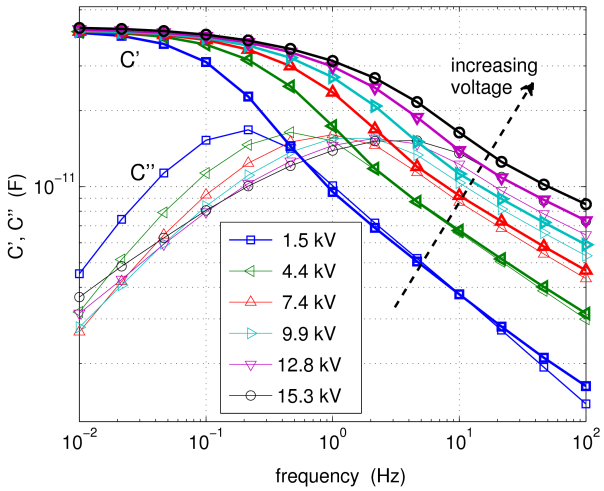

Figure 3. Currents measured in the taped bar's two graded ends: the fundamental-frequency components are displayed here as capacitance C' and loss C''.

Note that throughout this paper amplitudes given for sinusoidal voltages or currents are peak values.

In order to obtain the currents in just the graded parts the capacitance measured between the outer electrode and the inner tube, before the stress-grading material was applied,

was used together with the amplitude and frequency of the applied voltage to calculate the current to subtract from the measurements. The capacitance was treated as a real constant since PTFE has such low dispersion: the greatest frequency-dependence seen when measuring this capacitance over four decades of frequency was due to the instrument changing its feedback components, a variation of around 30 fF in 35 pF; the loss was also around 30 fF. Subtraction of this capacitance to give results for the graded part alone is important not only to make the changes more visible but also to emphasize some fundamental relations of C' and C'' in the 'dielectric response' of the grading's current. A slight error in the subtraction is probably the cause of the subpicofarad divergence of the 1.5 kV curves at the highest frequencies.

Several distinctive features can be seen in Figure 3. Towards low frequencies the capacitance tends to a constant irrespective of the amplitude of the voltage. This constant value is the capacitance of the PTFE insulation along the full length of the gradings: at a low enough frequency the conductance of the grading is high compared to the admittance of the insulation, and the zero-potential from the electrode at the start of the grading can spread all along the grading. The loss curves of Figure 3 have peaks that are shifted strongly up in frequency, and very slightly down in value, with increased voltage. A primitive description of the grading as a series RC circuit with a resistance that decreases with increased voltage, suggests that this shift to higher frequencies, i.e. to lower RC time-constants, is reasonable. At frequencies above the loss peak the capacitance and loss tend to straight lines: for the lower voltages these lines are not only parallel but are indeed superposed. More attention is given to this later, when discussing models.

3.2 HARMONIC CURRENTS

When the measured object is significantly nonlinear, as is the case here, the fundamental-frequency components of current in response to the sinusoidal applied voltage are only a part of the object's description. The harmonics in the current give an idea of the nonlinearity. In Figure 4 the magnitudes of harmonic currents of orders 3, 5 and 7 are shown, with values relative to the magnitude of the corresponding fundamental-frequency current.

Within the group at each ascending voltage, there are ascending frequencies, as annotated above the results of the 5th harmonic. Even-order harmonics are not expected, as the object has symmetric properties with respect to polarity: the magnitudes of the all even harmonics in current were well below the 7th harmonic shown here. The third harmonic reaches 15 % of the fundamental, and its relative value has much more dependence on the frequency than on the amplitude of the applied voltage over the reasonable dynamic range of these two parameters; higher frequencies imply higher electric fields at the start of the grading.

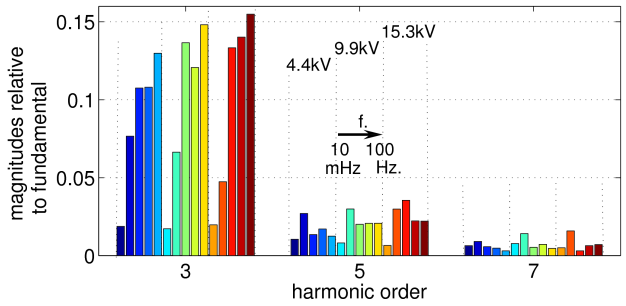

Figure 4. Amplitudes of the odd harmonic components of the current into the grading, *relative* to the fundamental-frequency component of current.

It was suggested in the introduction that the harmonic currents are mainly due to PD and stress-grading, and that being able to measure the pure PD current is one of the intended applications of this modeling. If PD is symmetric with respect to polarity, and is cavity-like in its phase so that the capacitive and lossy components of its current are of similar magnitude, it turns out that the relative sizes of the harmonics in the PD current are not clearly distinguished from those in an end-winding grading. The voltage-dependence of PD is however different, as the end-winding currents have significant harmonics even at quite low voltages that would be below the inception level of most PD sources. The frequency-dependence of PD is heavily dependent on the type of PD source [3]. Asymmetrical PD sources will produce some even-order harmonics that would not be in end-winding currents. These are possible means of distinguishing PD and end-winding currents in dielectric response measurements, but the removal of the end-winding current is still desirable.

4 MATERIAL DESCRIPTION

Before going on to numerical models of the whole grading construction the material properties of the nonlinear coating should be determined. Both the tape and the paint are based on SiC particles in a binding material. The tape has a woven backing, bearing the SiC together with a 'B-stage' epoxy that needs to be cured. It is the most conductive of the few types available from its manufacturer. The tape was used according to its instructions, being wound tightly half-lapped onto the PTFE tube and then cured for two hours at 160˚C. The paint was difficult to apply consistently, and it turned out that the thickness could easily vary enough to cause large (order of magnitude) changes in conductance. PTFE is a difficult substrate compared to real stator insulation.

4.1 LITERATURE ON THE MATERIAL PROPERTIES

The normal use of stress-grading is simply the prevention of excessive surface fields, without excessive loss. This puts no tight demand on the properties, and the materials' properties are therefore defined only very loosely by manufacturers. For simulation one would like to see an experimentally-based study of the relations of conductivity

and permittivity over a wide range of electric field and frequency, and an assessment of the variance in these properties with manufacturer, impregnation, aging etc. Previous investigations of end-winding grading have been interested in the heating-effect of the loss, or the distribution of electric field, particularly at frequencies much higher than the line-frequency such as when a switching inverter is used to drive a high-voltage motor [4, 5]. Investigations of slot and end-winding corona-protection materials are reported in [6], but the emphasis is still on the normal function of the material. For a density of axial current of about 80 nA/mm around the circumference, an acceptable range of surface-resistivity[1] is given as 2.5 GΩ/sq to 4.0 GΩ/sq (included in Figure 6 for comparison), but the material is not characterized under the range of stresses that is needed for modeling.

There is a close relation to the study of grading systems with similar purpose in medium-voltage cable terminations, where again the higher-frequency fields and heating are the main interest. The cable terminations also use powders, such as carbon-black or SiC, but distributed less densely, in a polymer matrix. Two simple forms of conductivity σ as a function of electric field E are widely found in published models. One is the power-law or 'varistor' equation of the form $\sigma(E) = kE^n$, used in studies of SiC-loaded insulators [7] cable-terminations [8] and end-windings [9], and in a more numerically friendly form having finite conductivity at zero field [10] also applied to cable-terminations. The other is the exponential relation of the form $\sigma(E) = k \exp(nE)$, widely used for end-windings [11, 12, 4, 2, 13] and having inherently good numerical properties of not vanishing at zero field. This has also sometimes been used for cable-terminations [14, 15].

It is clear that these two types of function cannot fit the same data well except for over a very limited range, and yet both are being used in each of two applications of SiC-based stress-grading. There is no substantial experimental data given in the above references to justify their material models over ranges of E relevant to stress-grading models.

In [16, 17] the electrical properties of SiC powders are studied in very good detail of conductivity and permittivity over a wide range of electric fields. The plotted results for conductivity suggest a function somewhere between the power-law and exponential ones, but one cannot justify the direct application of these results to stress-grading materials involving a binder material and possibly different size and doping of the SiC particles. In [18] and some later works on end-windings, a different equation is given, having properties that are a hybrid of the power-law and exponential forms

$$\sigma(E) = \sigma_0 \exp\left(n\,|E|^{2/3}\right) \quad (1)$$

where σ_0 is the zero-field conductivity; this is claimed to fit well to a range of end-winding grading materials. It has been found to fit well to our results, a lot better than either of the pure functions. Conductivity data from [17] were also found to be fitted well by equation (1).

4.2 MATERIAL MEASUREMENTS

The properties of the tape and paint materials were measured by applying a dc voltage up to 3 kV across coatings of the materials between copper-tape electrodes on PTFE tubes of 30 mm diameter, and measuring the resulting current with a Keithley 617 electrometer. The tube with samples of tape is shown in Figure 5.

Figure 5. A PTFE tube with four sample-lengths of the stress-grading tape between electrode pairs.

Electrode separations of 10, 20, 40 and 80 mm were used for the tape. By using different lengths it was possible to check that the current was very closely dependent on the ratio of applied voltage to length, and therefore that there was good contact between the electrode and the grading material right at the edge of the electrode. The thickness of the cured tape was about 0.5 mm, consistent between all the samples. Electrode separations of 10 mm were used for the paint, but because of the obvious variability of the paint's thickness three different samples were made, with intentionally different thickness. All were too varied in their thickness for a meaningful thickness to be reported; even the thickest layer of paint was thinner than the tape.

At low fields, particularly with the higher surface-resistivity of the thin paint, the current took even as much as tens of seconds to fall to the steady value determined by the resistive rather than the capacitive potential-gradient. At high fields the current increased, continuously over tens of seconds, perhaps due to heating of the material in spite of the very low power involved. In all cases the recorded current was the lowest value observed,: this gives the steady resistive current at low fields and the current before significant change in the material's state at high fields.

Figure 6 shows the results of measurements on the three thicknesses of paint and on the four lengths of tape, each measured on two occasions. Fitting to the data is done using equation (1) to relate the current I along the axis of the tube to the per-unit-length conductance at zero-field G_0 and the mean applied electric field $E=V/l$ where V is the applied voltage and l the length of the sample between the electrodes. This gives the equation

$$I = E\,G_0 \exp\left(n\,|E|^{2/3}\right) \quad (2)$$

whose parameters G_0 and n are shown in table 1 for each of the materials.

1 Surface-resistivity: the resistance between opposite sides of any square slab of the surface: this depends on material (bulk) resistivity and surface thickness, and is independent of the size of the square. It is a useful description for situations where the current runs along a layer whose thickness as well as material are fixed. The unit is Ω as opposed to Ω m for bulk conductivity, and is sometimes written 'Ω /sq' to emphasize that it is a general property of the surface rather than a particular object's resistance.

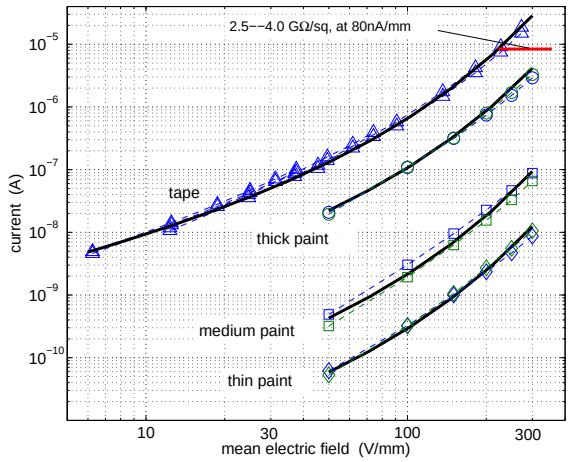

Figure 6. Measurements (triangular markers and dashed lines) along stress-grading materials applied between electrodes on a PTFE tube. The thick black lines fit (2).

The curves' parallel appearance makes it clear that it is mainly σ_0 that differs between them. Their shape has a clear upwards curve in the log-log scale (and had clear downwards curve in log-lin scale), indicating the inappropriateness of the widely used models.

Table 1. Material model parameters fitting equation (2) to Figure 6. The unit Sm, i.e. A/(V/m), is intended: it is the conductance of a 1 m length. The surface-resistivity at zero-field, $\rho_{\mathrm{surf}}(0)$ (Ω), is also derived, using the radius r of the PTFE tube.

Material	G_0 [Sm]	n	$\rho_{\mathrm{surf}}(0) = 2\pi r/G_0$
Tape	5.5×10^{-13}	0.00115	1.7×10^{11}
Paint (thin)	2.5×10^{-16}	0.00114	3.9×10^{14}
Paint (medium)	1.8×10^{-15}	0.00115	5.4×10^{13}
Paint (thick)	1.0×10^{-13}	0.00110	9.7×10^{11}

5 NUMERICAL MODELS

The numerical model that is used at the end of this section is based on a one-dimensional distribution of constant shunt capacitance and of nonlinear series resistance having the field-dependence described in the previous section. This type of model has been used in other work cited in the previous section, in studies of stress-distribution and heating at frequencies well above line-frequency. Its limitations when the potential changes rapidly in the axial direction, as happens at high frequencies, are discussed in [10]. The frequencies of interest to us are mainly at or below line-frequency, so the use of this model and omission of series capacitance is more easily justified than in these other works. On the way to this model, several simpler steps with less detail are used, explaining the features seen in the experimental results for the variation of C' and C'' with voltage amplitude and frequency. The models consider a single grading, one end of the laboratory objects. Only the 'tape' grading material is used for comparisons with the models, as it had so much better-defined thickness than the paint.

5.1 LINEAR, DISCRETE

A very simple model of the grading is a single discrete resistance and capacitance in series. The current into this arrangement, seen in the usual form of capacitance and loss, therefore appears as the Debye response. As the model is linear there is no voltage-dependence of the curves. A simple first step to modeling the nonlinearity is to let the resistance depend on the amplitude, but not on the instantaneous value, of the applied voltage.

As an example a capacitance of 21.3 pF was used, which is the total capacitance of the PTFE tube under the 80 mm length of the grading, excluding fringing. A resistance of 145 GΩ was chosen, which is the zero-field resistance of the 80 mm grading length. Figure 7 shows the capacitance and loss according to the linear discrete model with these values (dotted lines), then further cases where the resistance is reduced by factors of 10 and 100 to model higher applied voltages: these factors were chosen to give quite similar shifts to those observed in the experimental results.

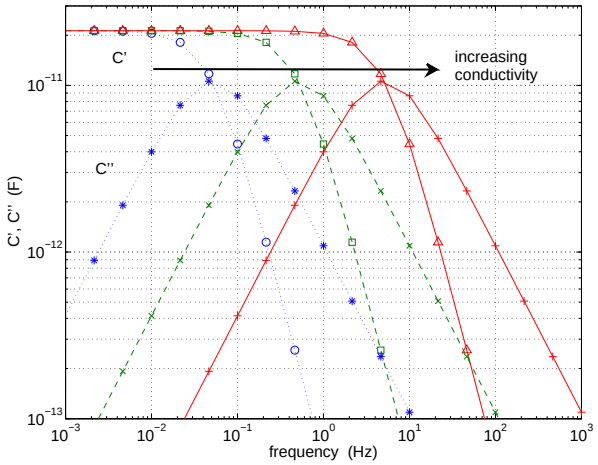

Figure 7. Capacitance and loss from the linear discrete model. The initial resistance (dotted line) is decreased by factors of 10 (dashed line) and 100 (solid line), to represent variation of conductivity with applied voltage

Towards high frequencies the slopes are much too steep compared to the experimental results, being Debye slopes where C' and C'' fall off at slopes of −2 and −1 'decades per decade'. The experimental results had both slopes around −0.5 at low voltages, and at higher voltage they were even shallower. The loss peaks move up in frequency but do not change in height or shape as the resistance is decreased.

Towards low frequencies the electric field in the grading is so low that the conductivity is near its zero-field value and is not much dependent on the applied voltage. The experimental results show this in how the loss curves at different voltages converge towards low frequency; the fixed resistance used here for each applied voltage cannot show this effect.

5.2 LINEAR, DISTRIBUTED

The linear discrete model, above, can have more and more RC sections joined to each other, to make a network of sections having series resistors and parallel capacitors, as in the discrete case of Figure 10. The result then tends to the distributed case, looking more like the experimental results at the higher frequencies. When the frequency is high enough that a single discrete section has a significant part of the voltage dropped across it, the results tend to the shape of the results from the discrete model.

For the linear case it is easy to solve the distributed model, using the generalized transmission-line equations in the frequency-domain, which permit arbitrary complex-values of series impedance and parallel admittance in each elemental length of the line [19]. Several previous users of this method are listed in [2]. A transmission-line approach is described there, and in [20] which gives the treatment used in the following paragraph.

The grading is a short length of transmission line, with a sinusoidal voltage applied at its near end (left, Figure 2) and an open circuit or lumped capacitance at its far end. A simple choice of components has just a series resistance R and parallel capacitance C. The closest standard transmission line value [19] to the desired output value of input current or complex capacitance is the input impedance Z_{in},

$$Z_{\text{in}} = Z_0 \frac{Z_{\text{end}} + Z_0 \tanh(\gamma l)}{Z_0 + Z_{\text{end}} \tanh(\gamma l)} \tag{3}$$

where l is the length of the line (grading), Z_{end} is the impedance terminating the far end, and the characteristic-impedance Z_0 and propagation constant γ are given by

$$Z_0 = \sqrt{\frac{Z_{\text{s}}}{Y_{\text{p}}}} = \sqrt{\frac{R}{j\omega C}}$$
$$\gamma = \sqrt{Z_{\text{s}} Y_{\text{p}}} = \sqrt{j\omega C R}$$

in which R and C, and therefore Z_{s}, Y_{p}, and γ, are all values per unit length. In a simple open-ended model (3) needs to be cancelled to

$$Z_{\text{in}} = \frac{Z_0}{\tanh(\gamma l)} \quad (\text{when } Z_{\text{end}} = \infty) \tag{4}$$

Any function of frequency can be used in Z_{s} and Y_{p}. For example, C may be a complex capacitance including frequency-dependence and loss, or a capacitance may be included in parallel with R to model the permittivity of the grading material and its surrounding. The simple RC case is treated here because it extends the linear discrete model in just one way. The situation thus described is diffusion rather than the wave-propagation that occurs when there is significant series inductance. With typical grading parameters the speed at which the applied voltage spreads along the grading is very slow, as is seen from the experimental results that show the low frequencies, and therefore the long periods, which the applied voltage must have before the end of the grading becomes significant and causes C' to reach a constant value.

The complex capacitance is found from Z_{in} as

$$C' - jC'' = \frac{1}{j\omega Z_{\text{in}}}, \tag{5}$$

which for the open-ended case with just R and C becomes

$$C' - jC'' = \sqrt{\frac{C}{j\omega R}} \tanh\left(l\sqrt{j\omega C R}\right) . \tag{6}$$

Using the same R and C values as for the linear discrete case, distributed over the 80 mm length of the grading gave the results shown in Figure 8.

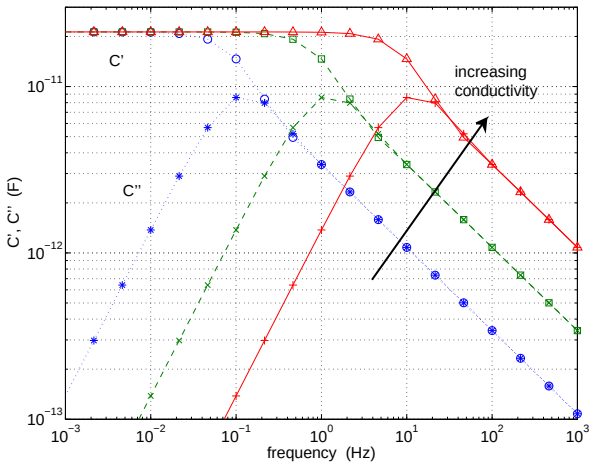

Figure 8. Capacitance and loss from the linear distributed model. The factors used to scale the conductivity are as in Figure 7.

There is much better fit to the experimental results around the high-frequency parts. The reason for the slope of –0.5 is clear from (6), where the tanh term tends to a real value of 1 as its argument grows, with the other term including $\omega^{-½}$ to give the slope and $j^{-½}$ to split this equally between real and imaginary parts. This special case of the 'universal law', with n=0.5, is mentioned in [21]; the slope is true for any infinite network of constant series resistance and parallel capacitance, independent of the actual values R and C. For the finite length of our practical case, the infinite network is a good approximation as long as the potential from the input end doesn't significantly change the potential at the far end. In the low-voltage experimental results this is true down to about 1 Hz, but then the end of the grading starts to be reached by the diffusion within each period of the applied voltage, and the results become similar to the linear discrete case, deviating considerably from those in the measurements. The linear discrete and distributed cases differ from each other quantitatively at the low frequencies, as the effective resistance is higher in the discrete case where the total capacitance was lumped at the end of the total resistance. This could be improved by scaling the resistance, but both linear models were only intended to give qualitative comparisons.

At high voltages the experimental results showed that the material behaves sufficiently nonlinearly that it does not show this n=0.5 response: the values of C' are shifted higher

than C'', and the gradient is less steep, both of these features corresponding to n>0.5 in the universal law. The grading cannot at high voltage be modeled as having the parameter R constant along its length.

5.3 NONLINEAR, DISCRETE

The effect of nonlinearity, but without the distributed RC nature, can be seen by replacing the discrete resistor with a conductance having voltage-dependence that follows the material conductivity equation (1). The total capacitance and total zero-field series resistance of the 80 mm grading were used here, as in the linear discrete model.

With a sinusoidal applied voltage v_{in} across the series-connected capacitance C and nonlinear resistance of zero-voltage resistance R, the voltage v_c across the capacitor is the state-variable in an ODE,

$$C\frac{\mathrm{d}v_c}{\mathrm{d}t} = (v_{in}-v_c)\frac{1}{R}\exp\left(n\,|v_{in}-v_c|^{2/3}\right) \quad (7)$$

This was solved numerically, using the `ode45` ODE solver in Matlab 7.5. The current into the grading is provided by the same solution, as it is the right-hand side of (7). The initial condition was v_{in}=0; the calculation was run for four cycles to reach an equilibrium, then the current at 32 evenly-spaced times was saved from each of the next two cycles. An FFT was performed to obtain the capacitance and loss as well as the low harmonics. The whole calculation was repeated over a range of amplitudes and frequencies of v_{in}. The results are shown in Figure 9.

Towards higher frequencies excessively steep gradients are seen, as in the linear discrete model. The heights of the loss-peaks do show a slight increase at lower voltages, as in the experimental results. The main improvement that has happened here, compared to the linear discrete model, is the convergence of the values of C'' towards low frequency; the nonlinear model has less voltage across the nonlinear resistance when at lower frequencies.

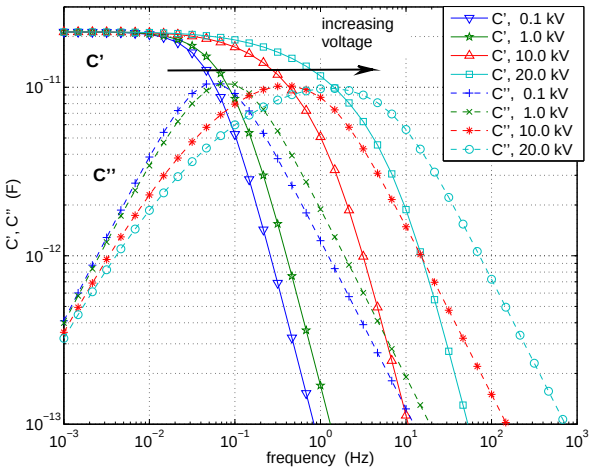

Figure 9. Capacitance and loss from the nonlinear discrete model.

5.4 NONLINEAR, DISTRIBUTED

The final model, combining the properties of nonlinearity and distributed parameters, is shown in Figure 10 as a parenthesized section that may be treated as an elemental length dx.

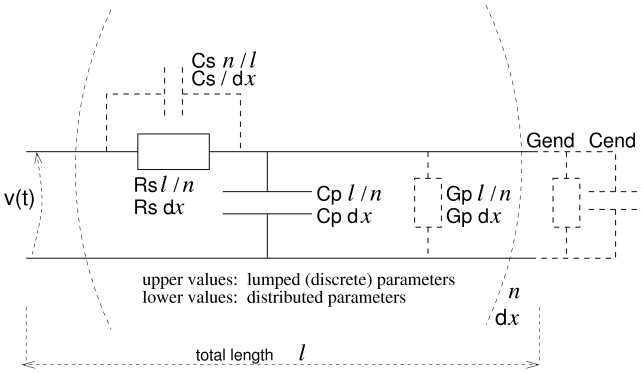

Figure 10. A one-dimensional model of a grading system. The part in parentheses may be discrete components repeated n times in a discrete model, or just an elemental section in a distributed model. R and C components within the parentheses are per unit length values. At least R_s may be nonlinear.

Beyond R_s and C_p, which have been used in the previous models, there are optional components that represent permittivity of the grading and its surrounding in C_s, loss in the insulation in G_p, and discrete components at the end to allow for fringing of the field or conductivity there. Variations of all of these, including nonlinearities, have been tried, along with variations in the material model's parameters. No single change had a large benefit to the fit to the measured results without also worsening the fit in other parts of the range of frequencies. The simple model using just directly-measured dimensions, with material properties from the material samples, has therefore been used here rather than arbitrarily adjusting the many possible parameters for a better fit of the measured results.

An analytical solution for the desired frequency-domain currents is not feasible with the nonlinearity and the possible extra components such as C_s and those at the end. Numerical solution is easily done. A solution is needed for the potential v, which is a function of time t and the position x along the grading from the zero-potential end to the open end. For simplicity of expression, the high-voltage conductor of Figure 2 is regarded as zero potential, and the end of the conductive outer electrode at the start of the grading is regarded as the negation of the actual applied voltage, so that the lower conductor in Figure 10 is at 0 V. The boundary conditions are then an applied sinusoidal voltage as a Dirichlet condition at the start of the grading x=0, and at the far end a Neumann condition of zero current for an open grading, or a mixed condition if including the lumped 'end' components.

When just R_s and C_p are used, and R_s is nonlinear according to (1) with zero-field value R_{s0}, the PDE describing this system is

$$C_p\frac{\partial v}{\partial t} = \frac{\partial}{\partial x}\left(\frac{\partial v}{\partial x}\frac{1}{R_{s_0}}\exp\left(n\left|\frac{\partial v}{\partial x}\right|^{2/3}\right)\right) \quad (8)$$

The solution was implemented in the pdepe PDE-solver in Matlab, with a spatial mesh of 32 points. A FEM-based solver in Comsol Multiphysics was necessary instead, when implementing some more complex details such as C_p, but it required tight tolerance settings for convergence and took longer, so was used only when necessary. Initial conditions of zero-potential everywhere were chosen. As with the nonlinear discrete model, calculation was run for four cycles to reach an equilibrium, then the results from the next two cycles were used as input to an FFT. The currents flowing into the grading were calculated from the 'flow'-term of equation (8), i.e. the term inside the outer parentheses of the right-hand side. The whole calculation was repeated for each amplitude and frequency. The values of C_p and zero-field R_s from the previous models were used, both given as values per unit length. The length of grading was 80 mm. The results are shown in Figure 11.

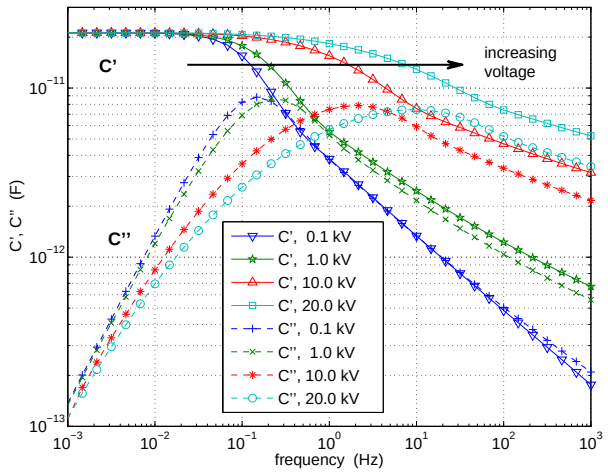

Figure 11. Capacitance and loss from the nonlinear distributed model.

All but one of the main features of the experimental results of Figure 3 are qualitatively reproduced here. The one missing feature is the increased C' and C'' at the higher voltages when moving to the lowest frequencies. This probably has an origin outside the basic properties of the material and geometry of a grading, such as PD or surface conductance on the insulator at the far end of the grading. When the earth-potential spreads to the far end, there will be strong electric fields around the grading's edge. At 10 mHz the rise in C' and C'' from lowest to highest voltage was seen in the experimental results to be about 2 pF.

For direct comparison of the experimental results and the nonlinear distributed model, curves for measured and calculated values at just three voltage points are plotted in Figure 12 with the calculated values doubled to match the double-ended bars. At frequencies above the loss-peak the difference between the measured and calculated results are all in one direction, the measured values being lower than the calculated values: from Figure 8 it can be surmised that this could be a consequence of an excessively high material conductivity used in the calculation.

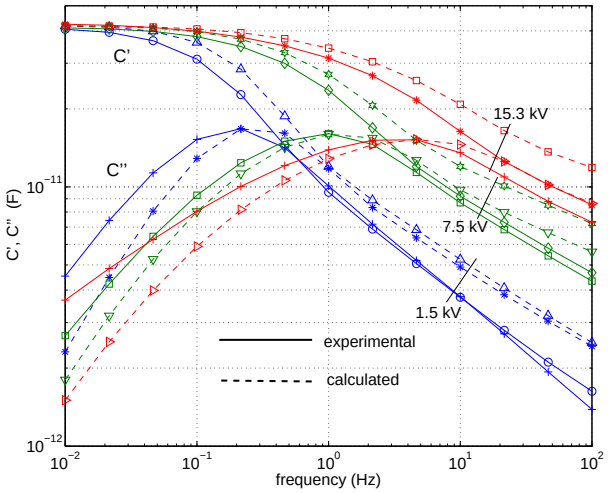

Figure 12. Comparison of capacitance and loss between measurement and the nonlinear distributed model.

6 DISCUSSION OF RESULTS

There are several differences between the laboratory models and real stator end-windings. Most important is the capacitance per unit square between the inner conductor and grading surface. For real stator insulation around the 10 kV level, with a thickness of a few millimetres and relative permittivity around 4.5, this capacitance is several times higher than for the PTFE tubes of thickness 5 mm and relative permittivity 2.1. Having a larger capacitance per unit length, without a correspondingly large increase in series conductivity, would shift the features of C' and C'' to lower frequencies. We are not aware of the availability of more-conductive stress-grading tapes than the one used here; some others from the same source have *lower* conductivity. The paint, even when quite thickly applied, had lower surface-conductivity.

The most important part of the curves for practical dielectric measurements is therefore at frequencies above the loss peak. In this range the far end of the grading is scarcely influenced by the potential at the stator end, and approximations of an infinite length are reasonable.

Having a distributed but linear model gave a better approximation at frequencies above the loss-peak than a discrete nonlinear model. The linear model, even if conductivity is uniformly scaled as some function of applied voltage, does not reproduce how at increasing voltages C' gets larger than C'' and their gradients get shallower, due to the higher conductivity in the higher-field region near the start of the grading. This behavior of C' and C'' would correspond to an increased slope in the time-domain in a linear power-law model of dielectric response.

The noncircular cross-section of stator bars, the proximity of bars from the same or other phases close to the graded section in an end-winding, and the possibility of significant dispersion or conductivity in the insulation material, are further differences between the laboratory models and real end-windings. On simple analyses these are not expected to be at all as important to the relevance of the

presented results as the difference in capacitance discussed above.

The harmonic content of the end-winding current increases with voltage amplitude and frequency, and reached as high at 15% of the fundamental for the third harmonic. Analysis of harmonics is a way in which end-winding current can be separated from the substantially linear current in the solid insulation, in the absence of PD. In the presence of PD currents particular features discussed in section 3.2 may be of some use for distinguishing end-winding and PD currents: measurements at voltages unlikely to have many active PD source, or PD sources with significantly different harmonic components or frequency-dependence from the end-winding currents.

Painted stress-grading material can clearly vary a lot in thickness. Even the taped material has been found [6] to vary with age or treatment, and various types are offered by several manufacturers. Accurate models of stress-grading currents are not practicable if one requires measured material properties and geometries from each machine: the grading material is hard to access even for visual inspection. It might be that a sufficient model for the substantial removal of the end-winding current in order to see the current due to PD can be achieved through estimation of the grading parameters using measurements at voltages below PD-inception, particularly if it could be shown that most of the model-parameters, such as the nonlinearity coefficient *n,* vary little between different machines.

7 CONCLUSION

Laboratory models have shown the features of the dielectric response current due to just the geometry and material of stator end-winding stress grading. The frequencies above the loss-peak are the most relevant to real end-windings, where the loss-peaks lie at much lower frequencies than in the laboratory models. At these frequencies C' and C'' at low voltage are similar to the case of a linear distributed-RC line, giving slopes of –0.5 decades per decade against frequency, but at higher voltages the slopes decrease and C' exceeds C'' as the nonlinearity changes the conductivity along the grading.

Towards lower frequencies where displacement currents in the insulation are small, the grading's conductivity starts to influence the potential at the grading's far end. This happens more easily if using lower frequencies, higher voltages, more conductive grading, less capacitive insulation, or if the grading is shorter. When the grading's end does become significant the dielectric response changes a lot, with the power-law curves seen for C' and C'' at the higher frequencies turning to more Debye-like curves that indicate a limit to the total charge that can move. The curves for C' tend to the capacitance that the whole length of grading would have if its material were conductive. As the electric field in the grading material is very low at low frequency, the nonlinearity becomes insignificant and the C'' curves also converge with each other as they diminish towards low frequency.

The linear discrete model fits poorly at all frequencies. The nonlinear discrete model using a single capacitor and nonlinear resistor gives a good approximation at frequencies below the loss-peak, which unfortunately is not of great practical interest. At frequencies above the loss-peak the linear distributed model is better than these other two models, but misses the separation of C' and C'' towards higher voltages. The nonlinear distributed model captures the main features below and above the loss-peak.

Descriptions of the nonlinear SiC-based grading materials were compared with measurements on our samples. It is clear that neither of the two commonly-used relations of conductivity to electric field is a good fit compared to a simple and numerically well-behaved relation that has been used in just a few recent works.

ACKNOWLEDGMENT

This work has been carried out within ELEKTRA project 36019, financed jointly by the Swedish Energy Agency, Elforsk, ABB and Banverket.

REFERENCES

[1] F. T. Emery, "Basics of power factor measurements on high voltage stator bars and stator windings", IEEE Electr. Insul. Mag., Vol. 20, No. 3, pp. 40–45, 2004.

[2] E. David and L. Lamarre, "Low-frequency dielectric response of epoxy-mica insulated generator bars during multi-stress aging", IEEE Trans. Dielectr. Electr. Insul., Vol. 14, No. 1, pp. 212–226, 2007.

[3] C. Forssen and H. Edin, "Partial discharges in a cavity at variable applied frequency Part 1: Measurements", IEEE Trans. Dielectr. Electr. Insul., Vol. 15, No. 6, pp. 1601–1609, 2008.

[4] F. P. Espino-Cortes, E. A. Cherney, and S. Jayaram, "Effectiveness of stress grading coatings on form wound stator coil groundwall insulation under fast rise time pulse voltages", IEEE Trans. Dielectr. Electr. Insul., Vol. 20, No. 4, pp. 844–851, 2005.

[5] J. C. G. Wheeler, A. M. Gully, A. E. Baker, and F. A. Perrot, "Novel stress grading systems for converter-fed motors", IEEE Electr. Insul. Mag., Vol. 23, No. 1, pp. 29–35, 2007.

[6] F. T. Emery, "The application of conductive and stress grading tapes to vacuum pressure impregnated, high voltage stator coils", IEEE Electr. Insul. Mag., Vol. 12, No. 4, pp. 15–22, 1996.

[7] A. Refsum, "Characterisation of SiC loaded insulators", IEEE Intern. Conf. Properties and Applications of Dielectric Materials (ICPADM), pp. 147–150, 1988.

[8] A. Roberts, "Stress grading for high voltage motor and generator coils", IEEE Electr. Insul. Mag., Vol. 11, No. 4, pp. 26–31, 1995.

[9] J. Rhyner and M. G. Bou-Diab, "One-dimensional model for nonlinear stress control in cable terminations", IEEE Trans. Dielectr. Electr. Insul., Vol. 4, No. 6, pp. 785–791, 1997.

[10] G. Lupo, G. Miano, V. Tucci, and M. Vitelli, "Field distribution in cable terminations from a quasi-static approximation of the Maxwell equations", IEEE Trans. Dielectr. Electr. Insul., Vol. 3, No. 3, pp. 399–409, 1996.

[11] J. P. Rivenc and T. Lebey, "An overview of electrical properties for stress grading optimization", IEEE Trans. Dielectr. Electr. Insul., Vol. 6, No. 3, pp. 309–318, 1999.

[12] H. El-Kishky, M. Abdel-Salam, H. Wedaa, and Y. Sayed, "Time-domain analysis of nonlinear stress-grading systems for high voltage rotating machines", IEEE Conf. Electr. Insul. Dielectr. Phenomena (CEIDP), pp. 482–485, 2003.

[13] L. Ming, F. Sahlén, K. Johansson, E. Mårtensson, H.-Å. Eriksson, O. Koponen, and S. Pääkkönen, "Effects of repetitive pulse voltages on surface potential distribution at end corona protection region of

high voltage motors", Intern Sympos. High Voltage Engineering (ISH), Paper No. T2–68, 2007.
[14] X. Qi, Z. Zheng, and S. Boggs, "Engineering with nonlinear dielectrics", IEEE Electr. Insul. Mag., Vol. 20, No. 6, pp. 27–34, 2004.
[15] V. Tucci and J. Rhyner, "Comment on "1-dimensional model for nonlinear stress control in cable terminations" [and Discussion and Reply]", IEEE Trans. Dielectr. Electr. Insul., Vol. 6, No. 2, pp. 267–270, 1999.
[16] E. Mårtensson, U. Gäfvert, and U. Lindefelt, "Direct current conduction in SiC powders", J. Appl. Phys., Vol. 90, No. 6, pp. 2862–2869, 2001.
[17] E. Mårtensson, U. Gäfvert, and C. Önneby, "Alternate current characteristics of SiC powders", J. Appl. Phys., Vol. 90, No. 6, pp. 2870–2878, 2001.
[18] A. M. Gully and J. C. G. Wheeler, "The performance of aged stress grading materials for use in electrical machines", IEEE Intern. Conf. Properties and Applications of Dielectric Materials, pp. 392–396, 2000.
[19] D. K. Cheng, *Field and Wave Electromagnetics,* Addison-Wesley, 1989.
[20] N. Taylor, "Diagnostics of Stator Insulation by Dielectric Response and Variable Frequency Partial Discharge Measurements", licentiate thesis, Kungliga Tekniska högskolan (KTH), Stockholm, 2006.
[21] A. K. Jonscher, *Dielectric Relaxation in Solids*, Chelsea Dielectrics Press, London, 1983.

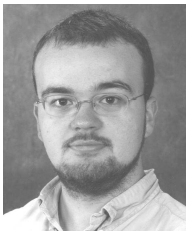

Nathaniel Taylor (S'02) was born in Oxford, England, in 1978. He received the M.Eng. degree in electrical and electronic engineering from Imperial College, London, in 2001. Since 2004 he has been employed as a research student at KTH in Stockholm, in the Insulation Diagnostics research group of the School of Electrical Engineering. His research area is the application to stator insulation systems of combined dielectric spectroscopy and partial discharge methods where the applied voltage is at a varied low frequency.

Hans Edin (M'08) was born in Sandviken, Sweden, on 16 April 1971. He received the M.Sc. and Ph.D. degrees in electrical engineering from the Royal Institute of Technology (KTH), Stockholm, Sweden, in 1995 and 2001, respectively. Presently his position is assistant professor at the Royal Institute of Technology. He is involved in research concerning development of insulation diagnostic methods for high voltage equipment. In particular, partial discharge analysis, dielectric spectroscopy and high frequency techniques for localization of degraded insulation.